Published in final edited form as:
Mol Cell. 2014 August 21; 55(4): 615–625. doi:10.1016/j.molcel.2014.06.025.

Frequent interchromosomal template switches during gene conversion in *S. cerevisiae*

Olga Tsaponina[1,2] and **James E. Haber**[1,2,*]

[1]Department of Biology, Brandeis University, Waltham, MA 02454-9110, USA

[2]Rosenstiel Basic Medical Sciences Research Center, Brandeis University, Waltham, MA 02454-9110, USA

Summary

Although repair of double-strand breaks (DSBs) by gene conversion is the most accurate way to repair such lesions, in budding yeast there is a thousand-fold increase in accompanying mutations, including interchromosomal template switches (ICTS) involving highly mismatched (homeologous) ectopic sequences. Although such events are rare and appear at a rate of 2×10^{-7} when template jumps occur between 71% identical sequences, they are surprisingly frequent (0.3% of all repair events) when the second template is identical to the first, revealing the remarkable instability of repair DNA synthesis. With homeologous donors, ICTS uses microhomologies as small as 2 bp. Cells lacking mismatch repair proteins Msh6 and Mlh1 form chimeric recombinants with two distinct patches of microhomology, implying that these proteins are crucial for strand discrimination of heteroduplex DNA formed during ICTS. We identify the chromatin remodeler Rdh54 as the first protein required for template switching that does not affect simple gene conversion.

Introduction

Although eukaryotic cells suffer multiple spontaneous chromosomal double-strand breaks (DSBs) every time they replicate their genome, homologous recombination mechanisms preserve the integrity of the genome. DSBs can be a product of natural replication process when replication fork collapses due to DNA lesions, physical impediments or dNTP pool depletion (Branzei and Foiani, 2010; Poli et al., 2012). Such stalled or broken forks can be restarted or rescued by the number of homologous recombination mechanisms (reviewed by (Yeeles et al., 2013). Recently attention has been focused on recombination coupled to replication that result in changes in gene copy number variation (CNV) and in remarkable complex chromosomal rearrangements known as chromothripsis in mammalian cells (Forment et al., 2012).

*Correspondence: haber@brandeis.edu.

A DSB can be repaired by using an identical, unbroken sister chromatid or identical or nearly identical sequences found on a homologous chromosome or at an ectopic location. One well-studied example of DSB repair by an ectopic donor is *S. cerevisiae* mating-type gene switching. Mating type is dictated by expression of **a** or α alleles at the *MAT* locus located on chromosome 3 (Chr3). *MAT* can switch to the opposite mating-type by gene conversion repair of a site-specific DSB induced by HO endonuclease, using one of two complete, but silent, donor copies – *HML* and *HMR* – located near telomeres on the same chromosome (reviewed by (Haber, 2012). Galactose-inducible expression of *HO* (Herskowitz and Jensen, 1991) creates a DSB in nearly all cells simultaneously in the population, allowing a detailed examination of DSB repair (Connolly et al., 1988; Hicks et al., 2011; White and Haber, 1990).

Recently we reported that while gene conversion is the most conservative pathway to preserve the genome, repair is associated with a thousand-fold increase in mutations in the newly copied DNA (Hicks et al., 2010). These mutations were detected during the gene conversion repair of an HO-induced DSB in *MAT* by using *Kluyveromyces lactis URA3* sequences embedded within the silent *HMR* locus (*hmr::Kl-URA3*). While gene conversion should produce a Ura^+ outcome, because the *Kl-URA3* sequences can be expressed at *MAT*, but not at *HMR*, Ura^- mutants can readily be selected. Many of these mutations have a distinctive signature, including frameshifts within homonucleotide runs, quasipalindrome alterations and – most surprising – interchromosomal template switches (ICTS) involving highly divergent copies of the template sequence. ICTS occurred when the nascent DNA strand dissociated from *hmr::Kl-URA3* and jumped to a different chromosome carrying the *S. cerevisisae*'s *ura3-52* allele, which is intact but not expressed because of a retrotransposon insertion at the 5' end of the gene. *Sc-ura3-52* is only 71% identical to *Kl-URA3*. Template switching requires a second jump back to the original *hmr::Kl-URA3* template to acquire the remaining sequences necessary to complete repair at *MAT*. ICTS as well as the other types of template switches resulted predominantly from errors of DNA polymerase δ (Hicks et al., 2010).

In the original study, only 2% of the Ura^- mutations arising during switching were ICTS. To study these events in much greater detail we modified the system so that only ICTS events would yield a selectable product, creating a functional chimeric *Kl-Sc-Kl-URA3* gene. This strategy enabled us to characterize the sizes of microhomology used in template switching and the extent of new DNA synthesis from the second template. We find that template switching is 10,000 times more frequently when the donor on Chr3 is completely homologous to the template on Chr5 than when it is homeologous, amounting to 0.3% of all recombination events. Deletion of the *RDH54* chromatin remodeler has no effect on normal DSB repair by gene conversion but reduces ICTS 70-fold; this is the first protein with a specific role in template switching. Our analysis of ICTS between homeologous sequences has also revealed novel roles for the Msh6 and Msh3 mismatch repair proteins in the discrimination of the template and nascent strands within heteroduplex DNA.

Results

Heterochromatin at *HMR* does not affect ICTS

To examine ICTS, we modified the previously described system so that other DSB repair events would be excluded (Fig 1A and 1B). Specifically, we deleted the *SIR3* gene, thus unsilencing *HMR*, and then created a 32-bp deletion in the *Kl-URA3* sequences inserted in *HMR* (*hmr::Kl-ura3-Δ32*), so that gene conversion repair of the HO-induced DSB at *MAT*α would result in Ura$^-$ outcomes, i.e. *mat::Kl-ura3-Δ32*. In contrast, an ICTS, in which a DSB repair event that began copying at *hmr::Kl-ura3-Δ32* but jumped to the homeologous *Sc-ura3-52* sequences on Chr5 and then back to *HMR*, could produce a Ura$^+$ outcome (Fig 1B). As shown in Table 1, we found that in a wild type strain lacking Sir3 the frequency of ICTS was similar to that estimated previously, about 2×10^{-7}. Because all of these events occur in a single cell division, these frequencies are equivalent to rates of recombination.

It was possible that dissociation of the newly copied strand during gene conversion from the heterochromatic *HMR* locus might result from difficulties in repair DNA synthesis caused by the ordered nucleosome structure of the donor (Weiss and Simpson, 1998). However, the heterochromatic state of *HMR* did not affect the rate of Ura$^+$ events and did not alter the sites of the homeologous junctions formed between *Kl-ura3* and *Sc-ura3* sequences nor the length of the *Sc-ura3* ectopic sequences copied (Table 1, Fig 1C and Table S1). Therefore we conducted the rest of our experiments in a *sir3*Δ background, which we will refer to as the wild type strain.

Perfect homology increases template switching

Interchromosomal switches between sequences sharing 71% homology occur rarely, about twice per 10^7 cells. We asked if the extensive mismatches between these donor templates pose a significant barrier to template jumps. We substituted *ura3-52* and its promoter with a promoterless *Kl-ura3* sequence also lacking the initial ATG codon, so that template switching would involve *hmr::Kl-ura3-Δ32* and a 100% identical *Kl-ura3* template on Chr5 (Fig 2A, compare i and iii). ICTS increased 10,000 times, to a rate of 3×10^{-3}, while spontaneous recombination measured between *mat::Kl-ura-Δ32* or *hmr::Kl-ura3-Δ32* and Chr5 *Kl-ura3* was 2.8×10^{-7} (Fig 2B, Table S2 and Table S3). Spontaneous recombination between two homeologous templates was lower than 1×10^{-10}.

We also inserted a donor with perfect *Kl-ura3* homology onto Chr3 between *MAT* and *HMR* in the same orientation as *HMR*, thus allowing us to examine *intra*chromosomal template switches (Fig 2A, compare iii and iv). The frequency of intrachromosomal template switches increased 3 times compared to ICTS (Fig 2B and Table S2). When a promoterless and ATG-less *S. cerevisiae ura3* gene was placed at the same location on Chr3 (Fig 2A, compare i and ii), the frequency of homeologous template switches increased 4 times compared to ICTS (Fig 2B and Table S2). With perfect homology, intrachromosomal template switching occurred in almost 1 in 100 gene conversion events (8×10^{-3}). This result reveals the remarkable instability of the repair DNA replication machinery during gene conversion.

ICTS can occur at many different homeologous junctions

To analyze the precise events that occurred in ICTS, we sequenced chimeric *URA3* genes at *MAT* after HO induction. In each case, the ICTS had copied the 32 bp missing from the *HMR* donor. The entry and exit points of each event (that is, the junctions on the 3' and 5' sides of the deletion, respectively) were determined by locating the regions of shared homology between the *Kl-ura3-Δ32* and *Sc-ura3-52* sequences. Both the entrance and exit points were spread over most of the *URA3* sequence (Fig 3A). Some junctions are much more preferred then others and are among the longest regions of microhomology, but other microhomologies of similar length are used much less often (Fig 3A–C and Table S1). The sizes of microhomology were not significantly different for entry and exit sites (Table 1); moreover there was no apparent relation between the exit sites used for any particular entry site. An example of the different exit sites used for one particular entry site is shown in Fig 3D. Among 142 examples analyzed from both *sir3*Δ and *SIR3* strains, the sequences copied from the *ura3-52* ectopic donor ranged between 76 and 412 bp, with a mean size of 246 and 247 bp, respectively (Table 1 and Fig 1C). Thus the heterochromatic state of the *HMR* donor did not alter the spectrum of repair events.

Genes involved in heteroduplex rejection and mismatch repair do not affect the rate of ICTS

Several types of homeologous recombination, including gene conversion, are inhibited by mismatch repair proteins and the Sgs1 helicase via heteroduplex DNA rejection (reviewed by (Boiteux and Jinks-Robertson, 2013). We tested whether deletions of different genes involved in heteroduplex rejection and mismatch repair, as well as the 3' to 5' DNA helicases, Sgs1 and Mph1, affected the efficiency of ICTS (Table 1). None of the tested mutants exhibited more than a 2–3 fold increase or decrease in ICTS rates, confirming that mismatch repair proteins are not predominantly responsible for the barrier to recombinat ion between highly diverged sequences (Dutta et al. 1996). Our observations do not allow us to determine if the rules for template switching between non-identical sequences are distinctly different from those governing initial strand invasion in gene conversion. We note that the lengths and distribution of microhomology junctions for template switching do not differ significantly from the wild-type strain in any of these mutants (Table 1, Fig S1A and S1B and Table S1). The strains lacking helicase activities had fewer short tracts (Fig S1B); however, none of the distributions was significantly different from the tracts in the *sir3*Δ strain ($p > 0.05$).

Deletion of *MSH6* leads to multiple patches after gene conversion repair

Despite the fact that deleting *MSH6* increased the rate only 2 fold and did not affect the general characteristics of ICTS events (Table 1 and Table S1), we were surprised to discover that 11% of *msh6*Δ Ura^+ clones possessed a chimeric *URA3* gene having two distinct patches of *ura3-52* sequence embedded in the *Kl-URA3* sequence at *MAT* (Fig 4A and Fig S2). One segment corrects the 32-bp deletion. The second *Sc-ura3* patch was found 3' of the deletion correction in 7 out of 8 of the cases, i.e. in sequences that were copied after the *MAT* end invaded *HMR* but prior to reaching the 32-bp deletion. These second patches were substantially shorter (19 to 64 bp) than those correcting the 32-bp deletion (mean length 231

bp; see Table 1). Such outcomes could be result of mismatch repair of a long heteroduplex formed after dissociation of the nascent repair strand from *hmr::Kl-ura3-Δ32* and invasion of this strand into *Sc-ura3-52* (Fig 4B). The remaining case had a second patch located 5' of the 32-bp correction (Fig S3) that could also reflect heteroduplex correction or a second ICTS. Similar *Kl-Sc-Kl-Sc-Kl-URA3* chimeric genes in *MAT* were found among 7% of Ura^+ outcomes from the *msh6Δ mph1Δ* strain.

Previously it was shown that heteroduplex loops (as opposed to single-bp mismatches) arising in meiotic recombination were repaired by a Msh2 and Msh3-dependent, but Mlh1 and Pms1-independent, process (Kearney et al., 2001). The patches of microhomology found in our study would produce a "bubble" of mismatched sequences rather than a single loop. In keeping with the idea that Msh3 would be required to introduce a second patch of *S. cerevisiae* sequences into the repaired product, we did not find any multiple patches in a *msh6Δ msh3Δ* double mutant. We also did not find any multiple patches among 94 isolates of the *msh6Δ mlh1Δ* double mutant. However, additional results presented below suggest that the *MSH3*-dependent multiple patches can be formed in the absence of Mlh1.

Deletion of *MSH6* or *MLH1* leaves a footprint in the ectopic *HMR* donor

Surprisingly, some of *msh6Δ* and *mlh1Δ* Ura^+ clones analyzed in the *sir3Δ* background, where *HMR* locus is unsilenced, should not have been Ura^+ because the sequenced *MAT* locus contained the *Kl-ura3* sequence harboring the 32-bp deletion. These clones could however be Ura^+ if the expressed *hmr::Kl-ura3-Δ32* locus had been converted to a functional sequence or if the *Sc-ura3-52* locus had somehow become reverted to *URA3*. Indeed, sequencing of *HMR* revealed that 4% of all Ura^+ analyzed in *msh6Δ* (4 out of 96) and 2% of the Ura^+ recovered in *mlh1Δ* (2 out of 96) had been converted to Ura^+ by the copying a segment of *Sc-ura3-52* to replace the 32-bp deletion at *HMR* (Fig 4C). The length of inserted sequence ranged from 127 to 322 bp. We believe these events are the result of mismatch repair after re-invasion of nascent strand dissociating from *Sc-ura3-52* and invading back into *hmr::Kl-ura3-Δ32*, followed by mismatch correction of the parental strand.

In the *msh6Δ mlh1Δ* double mutant, 3% of Ura^+ clones (3 out of 92 sequenced) had a footprint of *ura3-52* in *HMR*. No such footprints were found in 94 analyzed *msh6Δ msh3Δ* double mutants, compared to 6 of 118 examples where absence of Msh6 activity leads to *ura3-52* footprint in *HMR*. Altogether, 20 of 212 events in *msh6Δ* strains had either multiple *Sc-ura3-52* patches at *MAT* or a footprint of *Sc-ura3-52* in *HMR*. We conclude that Msh6 plays crucial role preventing such multiple events while Msh3 is required to establish them in the *msh6Δ* background. We suggest that these events can occur when cells fail to distinguish which strand is the intact donor and which is the incomplete nascent strand (Fig 4D).

To support our hypothesis that alterations of *HMR* or the multiple conversion tracts at *MAT* resulted from the repair of "bubbles" of mismatched sequences, we deleted *RAD1* in the *msh6Δ* strain, as the repair of heteroduplex loops has previously been shown to require Msh2-Msh3 and Rad1-Rad10 (Kearney et al., 2001). The absence of Rad1 did not affect the characteristics of ICTS but decreased survival, consistent with the role of Rad1 in removing

nonhomologous 3'-ended tails during *MAT* switching (Lyndaker et al., 2008) (Table 1, Table S1 and Table S4). Without Rad1, multiple patches of *Sc-ura3* in *MAT* and footprints of *ura3-52* in *HMR* were absent in *msh6*Δ strain a result consistent with a loop-repair mechanism.

All the above described events were likely due to the repair of the DSB in the *MAT* as the rate of spontaneous recombination between *Sc-ura3-52* and either *mat::Kl-ura3-*Δ*32* or *hmr::Kl-ura3-*Δ*32* where HO endonuclease cannot act was 0.7×10^{-10} (Table S3), compared to the HO-induced rate of about 2×10^{-8} ($0.04\times4.8\times10^{-7}$). Although a previous study found increased spontaneous recombination between diverged sequences in *msh3*Δ strains (Datta et al., 1996), we did not find any *Sc-ura3-52* patches in *MAT* or *HMR* in *msh3*Δ strain. We suggest that the multiple patches of *ura3-52* sequence at *MAT* or the Ura^+ conversions at *HMR* result from *MSH3*-dependent repair of extensive heteroduplex DNA formed in the absence of Msh6, as described above.

Overexpression of Rad51 does not affect ICTS in wild-type strain

MAT switching is eliminated in the absence of the recombination protein Rad51 or its interacting chromatin remodeler, Rad54 (Malkova et al., 1996; Signon et al., 2001). We confirmed here that *RAD54* is required for all HO-induced repair events (Table S4). Rad51 is a recombinase that catalyzes homology searching and strand exchange between homologous sequences (Renkawitz et al., 2013; Sung, 1994). Overexpression of Rad51 has been shown to increase the efficiency of break-induced replication (Lydeard et al., 2010). To investigate if increased levels of Rad51 might affect the frequency of ICTS, we transformed the wild type strain with a plasmid carrying *RAD51* expressed under a constitutive *PGK* promoter. Overexpression of *RAD51* had no effect on simple gene conversion, which was already >92% efficient with normal levels of Rad51. The rate of ICTS was also unaffected (Table S2).

Rdh54 is required for template switches

It is not evident if ICTS uses only the recombination machinery required for simple gene conversions; consequently we investigated the role of Rdh54 and Rad59 in this process as both proteins had been implicated earlier in a Rad51-independent repair mechanism (Ira and Haber, 2002). Rdh54 (Tid1) is a homologue of Rad54, but has distinct functions in DSB repair. Although it plays a major role in meiotic recombination in combination with the Rad51 homolog, Dmc1, it has very little effect on mitotic recombination (Holzen et al., 2006; Klein, 1997; Shinohara et al., 2000). Moreover, Rdh54, along with both Rad54 and a third homolog, Uls1, has been implicated in dissociating Rad51 from double-stranded DNA (Shah et al., 2010). We confirmed that deleting *RDH54* had no discernable effect on the very efficient repair of HO-cut *MAT*α with the *hmr::Kl-ura3-*Δ*32* donor, as simple gene conversion was not decreased (Table S4). It was therefore astonishing that ICTS in an *rdh54*Δ strain was decreased 70 fold compared to the wild type strain (Fig 5A and Table S2). Although the *rdh54*Δ mutant is adaptation-defective, when there is no repair, it is proficient in resuming cell cycle progression after repair (Lee et al., 2001). Nevertheless, to show that *rdh54*Δ was not defective in resuming cell cycle progression, we measured ICTS in an *rdh54*Δ *chk1*Δ strain where its checkpoint defect is suppressed. The frequency of ICTS

in such a strain remained as low as for *rdh54*Δ strain (data not shown) indicating that failure to produce Ura^+ colonies is not due to inability to resume growth after healing a DSB.

When the homeologous donor in *rdh54*Δ strain was placed on Chr3, *rdh54*Δ still inhibited template switching by a factor of 20 (Fig 5A, compare i and ii, and Table S2). The strong role of Rdh54 in ICTS was seen even when the Chr5 donor carried a fully homologous *Kl-ura3* sequence, where ICTS in *rdh54*Δ was reduced to 10% of the wild type level (Fig 5A and Table S2). When we moved a homologous donor to Chr3 in *rdh54*Δ strain the frequency of template switching was reduced 3 fold (Fig 5A, compare iii and iv, and Table S2). We conclude that Rdh54 is crucial for the DNA transactions during both inter- and intrachromosomal template switches between divergent sequences even though it has no significant role in simple gene conversion.

We asked if Rdh54's role was connected to two of its previously identified functions. Rdh54 plays a central role in meiosis with the Rad51 homolog, Dmc1, which should not be expressed in mitotic cells (Dresser et al., 1997; Petukhova et al., 2000). To be certain that Dmc1 was not involved, we measured ICTS in *dmc1*Δ and found no effect (Table S2 and Table S4). In addition, Rdh54 acts along with its homologs Rad54 and Uls1 to displace Rad51 from dsDNA (see above). Rad54 is essential for all DSB-provoked gene conversion (Table S4), but *uls1*Δ has no effect on gene conversion and ICTS (Table S2 and Table S4).

Spontaneous recombination measured between *Kl-ura3* on Chr5 and *mat::Kl-ura3-*Δ*32* or *hmr::Kl-ura3-*Δ*32* in *rdh54*Δ strain was similar to the wild type strain arguing that *rdh54*Δ cells are proficient for recombination but deficient for ICTS (Table S3). These data identify *rdh54* as the first mutation to specifically impair ICTS without affecting gene conversion *per se*.

Finally, we show that Rad59, another protein implicated in a Rad51-independent recombinational repair process (Ira and Haber, 2002), is also important for ICTS (Fig 5B). However, unlike *rdh54*Δ, deletion of *RAD59* also affects the efficiency of gene conversion, reducing it to about 30% (Table S4). Spontaneous recombination between two identical sequences in both *rad59*Δ and *rad59*Δ *rdh54*Δ strains were also lower than in wild type (Table S3), whereas deletion of *RDH54* does not affect either gene conversion or spontaneous recombination.

The frequency of ICTS between homeologous sequences was reduced 9 fold in *rad59*Δ compared to the wild type (Fig 5B, system i). ICTS between homologous sequences was also reduced 9 fold compared to wild type, from 3.0×10^{-3} to 3.7×10^{-4} (Fig 5B and Table S2). This reduction is comparable to that seen with *rdh54*Δ (3.4×10^{-4}). When we deleted *RDH54* in the *rad59*Δ background, the rate of ICTS between homologous sequences decreased a further 3 fold, arguing that deleting these two genes may affect more than one pathway (Fig 5B and Table S2).

ATPase activity and interaction with Rad51 are important for the role of Rdh54 in template switching

Rdh54 is ATP-dependent DNA translocase and interacts with Rad51 protein through its N-terminus (Chi et al., 2006; Santa Maria et al., 2013). To elucidate if translocase activity or interaction with Rad51 is required for template switch, we transformed *rdh54*Δ strain with plasmids carrying full-length *RDH54* (pHK489), *rdh54* lacking first 75 amino acids required for interaction with Rad51 (pHK549) or *rdh54-K318R* (pRB101), all expressed from their native promoter (Santa Maria et al., 2013). Full length *RDH54* restored ICTS to the wild-type level, while neither *rdh54-*Δ*75* nor *rdh54-K318R* constructs were able to rescue the *rdh54* phenotype (Fig 5C and Table S2). We conclude that both ATPase activity and interaction with Rad51 are required for ICTS during gene conversion repair.

As the Rad51-interacting domain of Rdh54 is required for ICTS, we asked if overexpression of Rad51 would affect ICTS in the *rdh54*Δ strain. As constitutive overexpression of *RAD51* is deleterious in a *rdh54*Δ strain ((Santa Maria et al., 2013) and data not shown), we transformed *rdh54*Δ with galactose-inducible *RAD51* on a multicopy plasmid pHK317(3) (Santa Maria et al., 2013) and simultaneously induced a DSB and *RAD51* overexpression for five hours. Transient Rad51 overproduction did not affect the rate of ICTS in the *rdh54*Δ strain (Table S2), but significantly reduced its survival to 47% compared to the *rdh54*Δ strain transformed with an empty vector (Table S4). Finally, we found that overexpression of *RDH54* under a native promoter from a multicopy plasmid (pOT23) did not affect ICTS (Table S2).

The kinetics of the first and second template switches are similar

We analyzed the timing of intrachromosomal jumps by semi-quantitative PCR analysis. Appropriate dilutions of template DNA were assessed by the intensity of PCR bands that were quantified after agarose gel resolution (see Experimental Procedures). We designed a set of primers to detect kinetics of the simple *MAT*α → *mat::Kl-ura3-*Δ*32* switch (Fig 6A). Two other primer pairs were created to detect (a) the copying of the 32-bp segment after *MAT* end invaded into *Kl-ura3 donor* and (b) the completion of template switch, when the 32-bp region from *Kl-ura3* was joined to *MAT*-proximal sequences (Fig 6A).

In the homologous intrachromosomal system (Fig 6B) the kinetics of the simple gene conversion was similar to those described previously (Hicks et al., 2011): the PCR product for primer extension and the repaired product at *MAT* were detected as early as 1 h after HO cut and DSB formation (Fig 6C). Repair was complete by 6 h and nearly 100% of cells completed repair (Fig 6C).

The timing of both the first and second steps of template switch were similar to that much more abundant gene conversion repair product, suggesting that there are no long delays in the search for homology in template switching, and the second template switch immediately follows the first template switch (Fig 6C).

Discussion

Accurate repair of DSBs is essential to ensure genome stability. Although gene conversion – inserting a small patch of newly synthesized DNA to seal up a DSB – is a conservative way to accomplish repair, it is not without risk. There is a 1000-fold increase in mutations within the newly copied sequences (Hicks et al., 2010). Many of these mutations apparently result from dissociations of the partially copied strand from its donor template and then its inaccurate re-association, yielding frameshift mutations in homonucleotide runs, quasipalindrome mutations and – most remarkably – interchromosomal template switches between highly divergent templates. In this paper we have focused on ICTS and documented a number of remarkable aspects about its molecular mechanism.

One concern in our original work was that the initial donor sequences (*hmr::Kl-URA3*) were heterochromatic, so that it was possible that the high rate of ICTS was prompted by the difficulty in the repair DNA polymerase to copy these sequences, although normal *MAT* switching using these heterochromatic sequences is nearly 100% efficient (Haber, 2012). Here we show that ICTS is not significantly affected when the donor is unsilenced compared to the silent, heterochromatic state. These results suggest that neither the initial dissociation nor the re-invasion of the nascent strand after copying sequences from the interchromosomal donor is altered by the heterochromatic state of *HMR*.

ICTS between 71% identical templates was readily detectable by selection, and represented 2–4% of all the mutations we recovered (Hicks et al., 2010), but the rate of these interchromosomal jumps was only about 2 in 10^7 cells. We now find that this low rate reflects the barriers imposed by the extensive sequence divergence of the *K. lactis* and *S. cerevisiae URA3* sequences, because when the Chr5 donor was changed to be identical to the sequences in *hmr::Kl-ura3-Δ32*, the rate of ICTS increased 10,000 times, to about 3×10^{-3}. In fact when the donor was moved from Chr5 to Chr3, so that all the transactions were intrachromosomal, the rate of template switching was 8×10^{-3} (Fig 2B and Table S2). These kinds of template jumps vastly exceed the rates of simple frameshift or quasipalindrome mutations, which simply involve realignments of the nascent strand on a single template, which were found at a rate of about 3×10^{-5} (Hicks et al. 2010). Our results emphasize the remarkable instability of the repair replication process, such that nearly 1 in 100 events was accompanied by the pair of template jumps. We note that we only detect events that copy the region correcting the 32-bp deletion; there could easily be an equal or larger number of events that copied other segments of the template but would not be scored in our assay. In any case it is evident that ICTS is very common, indicating that DNA synthesis machinery is extremely unstable and prone to dissociation from a template strand. If we assume that the rate of dissociation from the template and invasion in a second donor is the same for both of the required two jumps to complete repair, then the rate of dissociation and ectopic invasion occurs once in every ten events.

Template switching was also described earlier in another type of recombination repair – break-induced replication (BIR), when invading strand turns to replication fork and continues DNA synthesis to the very end of a chromosome (Deem et al., 2008; Smith et al., 2007). Despite parallels between gene conversion repair and BIR, such as highly inaccurate

DNA synthesis (Deem et al., 2011; Hicks et al., 2010) and a conservative mechanism of DNA replication involving a migrating D-loop (Donnianni and Symington, 2013; Ira et al., 2006; Saini et al., 2013), the template switch machinery might be distinct from either of these two processes. First, we showed that GC-associated template switching is not affected by the overproduction of Rad51 recombinase, whereas ectopic BIR is increased (Lydeard et al., 2010). Second, single or double deletion of *MUS81* or *YEN1* endonucleases or *MPH1* helicase implicated earlier in BIR template switching (Pardo and Aguilera, 2012; Stafa et al., 2014), did not change rates of ICTS in our system (Table 1 and data not shown). Finally, we have previously shown that deleting *POL32*, which is required for BIR, has no effect on ICTS (Hicks et al., 2010).

The barriers to homeologous ICTS are formidable. We have knocked out many of the mismatch repair (MMR) genes and 3' to 5' helicases that have been shown to play some role in rejecting recombination between mismatched sequences, albeit usually less mismatched than the 71% divergence between the sequences used here (Alani, 1996; Nickoloff et al., 1999; Schmidt et al., 2006); none of them exhibited more than a two-fold increase in ICTS (Table 1). These results might mean that ICTS acts in a different fashion, not relying on the MMR genes and the helicases to prevent recombination. Indeed, it is not certain whether the jumps into and out of *ura3-52* require the Rad51-mediated strand exchange machinery. Heteroduplex rejection by MMR and helicases might only occur in the context of Rad51-mediated exchange and not if ICTS involved template switches mediated directly by the DNA polymerase still associated with the nascent strand. Alternatively, the extent of divergence might simply be too great for MMR proteins to act efficiently. In a previous study a *msh6*Δ mutant alone increased homeologous recombination between 91% identical sequences 4-fold and *msh6*Δ *msh3*Δ increased the rate almost 70-fold (Spell and Jinks-Robertson, 2003). A similar effect was shown for *msh3* and *msh2* mutants in recombination between 77% homologous sequences (Datta et al., 1996). However, in ICTS between 71% identical templates, neither *msh6*Δ nor the double mutant *msh6*Δ *msh3*Δ increased the rate by more than about 2-fold (Table 1).

The junctions formed during ICTS are characterized by small patches of microhomology. Many different junctions are used, with an average length of about 8–9 bp. Sites with the longest microhomology (11 bp on one side of the Δ32 deletion and 17 bp on the other) were used more frequently than any others, but sites with only 5–8 bp microhomology were also frequently used and some sites of only 2 bp were among the highest usage. Hence, we do not deduce a very clear rule about where strand invasions into and out of the homeologous template should take place. There also was no evident correlation between the site of invasion into *ura3-52* and the site of departure.

It should be noted that the site where we detect microhomology does not mean that the invasion of the displaced strand into the homeologous template was restricted to these few base pairs. A much longer region of heteroduplex DNA might be established and then acted upon by mismatch repair genes to yield a final outcome (reviewed by (Boiteux and Jinks-Robertson, 2013; Chen and Jinks-Robertson, 1998)). This idea is strikingly emphasized by a remarkable phenotype of deleting *MSH6*.

Although *msh6*Δ did not significantly change the rate of ICTS, the absence of this gene resulted in nearly 10% of all *mat::URA3* outcomes having 2 patches of *ura3-52* sequences in the final outcome, each bounded by microhomology junctions (Fig 4A and 4B, Fig S2 and Fig S3). Although these events could reflect four template switches instead of the normal two needed to replace the 32-bp deletion, we believe that these outcomes reflect the formation of a long region of heteroduplex DNA between the divergent sequences, followed by "patchy" mismatch repair. In the absence of *MSH6*, the length of heteroduplex might be much longer, affording loops of consecutively mismatched bases to be repaired by a Msh6-independent repair process. Indeed heteroduplex loops in meiotic cells have been shown to be repaired by an Msh3-dependent process (Kearney et al., 2001). Here, we find that the frequent instances of two-patch gene conversion in *msh6*Δ are eliminated in *msh6*Δ *msh3*Δ cells. We note that in the meiotic case, the heteroduplex was a single indel loop, whereas in the case we are examining, two mismatched unpaired strands of equal length will form symmetrical loops. The repair of such discontinuities appears to require not only Msh3 but also the Mlh1 (and presumably Pms1) proteins, which were not required for repair of the simpler meiotic loops.

The *msh6*Δ and *mlh1*Δ strains also displayed another previously unseen phenotype in which the cells were Ura^+ in spite of having copied the *Kl-ura3-*Δ*32* sequence into *MAT*. These unexpected cases proved to have one patch of *ura3-52* sequence copied into the transcribed *HMR* donor, creating a chimeric Ura^+ gene (Fig 4C). Among hundreds of wild type and other mutant strains that we have analyzed we found no cases where the *URA3* sequences were not at *MAT*. We believe these cases represent instances in which the displaced strand, leaving the *ura3-52* donor, forms an extensive heteroduplex at *hmr::Klura3-*Δ*32* which leads to mismatch repair of the *hmr::Kl-ura3-*Δ*32* sequence (Fig 4D). These events can only be obtained if cells fail to discriminate which is the nascent strand in two sequential steps during dissociation/strand re-invasion at *hmr::Kl-ura3-*Δ*32*, while for the formation of two *Sc-ura3* patches at *MAT* the lack of strand discrimination activity is not required. We conclude that Msh6 and Mlh1 normally play an important role not only in confining the length of heteroduplex but in directing mismatch repair to the nascent strand rather than the uninterrupted template. Further evidence of this "reverse" mismatch repair came from discovering cases in *msh6*Δ that had a chimeric and functional *URA3* gene at *MAT* but a patch of *ura3-52* sequences at the *HMR* donor as well. As at *MAT*, these unusual events were eliminated when Msh3 was deleted in the *msh6*Δ strain.

In addition to identifying novel roles for Msh6 in homeologous ICTS, we have discovered the first protein that is required for ICTS but has no evident role in simple gene conversions. Deletion of *RDH54* has no impact on simple gene conversion between *MAT*α and *hmr::Kl-ura3-*Δ*32*, but profoundly reduced ICTS. In the homeologous ICTS system *rdh54*Δ reduced events by 70 fold. In homologous inter- and intrachromosomal assays, *rdh54*Δ still reduced the rate of Ura^+ recovery by 10- and 3-fold, correspondingly.

In meiosis, Rdh54 is required for the efficient strand invasion activity of the Rad51 homolog, Dmc1 (Dresser et al., 1997; Petukhova et al., 2000). Dmc1 is not expressed in mitotic cells, but Rdh54 may adopt a similar role with Rad51 in these unusual

circumstances. Indeed our analysis showed that the *rdh54*-Δ*75* mutation which eliminates its interaction with Rad51 (Santa Maria et al., 2013) behaves as a null mutation (Fig 5C).

We do not yet know how Rdh54 might specifically facilitate ICTS, but it seems possible that Rdh54 is required to facilitate the strand invasions at the distant donor (Renkawitz et al., 2013; Sung, 1994). Alternatively, Rdh54 is required to dissociate nascent strand from either *hmr::Kl-ura3*-Δ*32* or *Kl-ura3* donor to execute either first or second template jump.

Experimental Procedures

Yeast strains and plasmids

All strains used in this study are isogenic to JKM153 (Hicks et al., 2010). Table S5 notes only the allele(s) that differ from the JKM153 genotype.

The 32-bp deletion (Δ*32*) in *Kl-URA3* was created by PCR mutagenesis using primers OT09, OT10, OT12 and OT13 (see Table S6). An *hmr::Kl-URA3* construct lacking the HO cut site was used a template (Hicks et al., 2010) to create *Y***a***::Kl-ura3*-Δ*32* cassette.

To introduce *Kl-ura3-KANMX*, *Kl-ura3-TRP1* or *Sc-ura3-KANMX* into Chr 3 or 5, a pRS315-based plasmids were created by *in vivo* recombination (Oldenburg et al., 1997) where *K. lactis* or *S. cerevisiae URA3* ORFs were placed adjacent to *KANMX* or *TRP1* markers resulting in plasmids pRS314-*pLEU2-Kl-URA3-KANMX6* (pOT04), pRS314-*pLEU2-Kl-URA3-TRP1* (pOT05) or pRS314-*pLEU2-Sc-URA3-KANMX*6 (pOT14). Appropriate PCR fragments were transformed into yeast strains (Table S6).

To express *RDH54*, *rdh54*-Δ*75* or *rdh54-K318R* from their native promoters, previously described plasmids pHK489, pHK549 and pRB101 were used (Santa Maria et al., 2013). To overexpress *RDH54*, a full length *RDH54* under its native promoter was PCR-amplified using pHK489 (Santa Maria et al., 2013) as a template and then inserted into the 2μ YEp13-*LEU2* vector (Broach et al., 1979) by *in vivo* recombination creating pOT23. To overproduce Rad51, the previously described pSJ5 was used (Lydeard et al., 2010).

Analysis of template switching frequencies and survival

Yeast cells were grown in YP media supplemented with raffinose to mid-log phase, induced 4 h with galactose, collected and appropriate dilutions were plated on YPD plates and plates lacking uracil. For survival analysis, an equal number of cells were plated on YP+Dextrose and YP+Galactose. Plates were incubated 3 days at 30°C and the number of colonies were counted. Three repetitions per strain were performed; 3 clones were analyzed per repetition.

To measure spontaneous recombination frequencies in different strains, a Ura$^-$ *MAT***a**-like strain (*mat::Kl-ura3*-Δ*32 hmr::Kl-ura3*-Δ*32*) was used. The HO-cut site is absent at both *mat* and *hmr*, therefore HO-induced events are excluded. Spontaneous recombination can occur between the ectopic donor on Chr5 and either *mat::Kl-ura3*-Δ*32* or *hmr::Kl-ura3*-Δ*32*; we scored total Ura$^+$ colonies and did not distinguish between the two loci. Frequencies were scored as described above.

Error bars indicate the standard error of the mean. To assess if difference between strains is significant, t-test analysis was performed.

Sequencing analysis of Ura$^+$ colonies

Genomic DNA was extracted from Ura$^+$ colonies with a MasterPure Yeast DNA purification kit (Epicentre) and *MAT* or *HMR* loci were PCR amplified using MATX_F + MATDp8, or OT09 + OT10 primers, correspondingly (Table S6). PCR products were sequenced with MATXp1 and KlUra3p1 primers, correspondingly. Chimeric *URA3* sequences were aligned against *S. cerevisiae URA3* and junction sites were identified at the border of homology.

Analysis of kinetics of template switches by semi-quantitative PCR

Yeast were grown in YP supplemented with raffinose to OD ≈ 0.4, nocodazole-arrested for 3 hours at 20μg/ml, and HO-induced by adding 2% of galactose. Approximately 2×10^8 cells were collected by centrifugation and DNA was purified with MasterPure Yeast DNA purification kit (Epicentre). DNA concentration was normalized according to PCR with primers to unrelated sequence *SLX1* (Table S6) and appropriate dilutions of a DNA were subjected to PCR with primers p1 (OT88), p2 (MATdist_2R), p3 (Kl URA3p1), p4 (OT70), p5 (OT71) and p6 (MATXp1). Three standards with known DNA concentrations were run in parallel. To avoid saturation of PCR products in test samples and standards, different number of amplification cycles were applied and DNA standards of different concentrations were used for every set of primers. To analyze simple gene conversion, samples were amplified for 20–22 cycles and standard DNA range 0.1×10^{-4}–1.0×10^{-4} pg/μl was used for primers p1 and p2 and 0.1×10^{-3}–1.0×10^{-3} pg/μl for primers p3 and p2. To analyze template switch, samples were amplified for 42–44 cycles and standard DNA concentration of 0.1×10^{-6}–1.0×10^{-6} pg/μl or 0.1×10^{-7}–1.0×10^{-7} pg/μl was used. DNA fragments were resolved by 2% agarose gel stained with ethidium bromide, checked for saturation with Quantity One 1-D software (Bio-Rad) and then quantified with same software.

Supplementary Material

Refer to Web version on PubMed Central for supplementary material.

Acknowledgments

We thank H. Klein for plasmids, N. Sugawara and other members of the Haber group for advice and discussion. OT is supported by an International postdoc fellowship from The Swedish Research Council, reference number 2011–6805. Research in the Haber lab is funded by NIH grants GM20056 and GM76020.

References

Alani E. The Saccharomyces cerevisiae Msh2 and Msh6 proteins form a complex that specifically binds to duplex oligonucleotides containing mismatched DNA base pairs. Mol Cell Biol. 1996; 16:5604–5615. [PubMed: 8816473]

Boiteux S, Jinks-Robertson S. DNA repair mechanisms and the bypass of DNA damage in Saccharomyces cerevisiae. Genetics. 2013; 193:1025–1064. [PubMed: 23547164]

Branzei D, Foiani M. Maintaining genome stability at the replication fork. Nat Rev Mol Cell Biol. 2010; 11:208–219. [PubMed: 20177396]

Broach JR, Strathern JN, Hicks JB. Transformation in yeast: development of a hybrid cloning vector and isolation of the CAN1 gene. Gene. 1979; 8:121–133. [PubMed: 395029]

Chen W, Jinks-Robertson S. Mismatch repair proteins regulate heteroduplex formation during mitotic recombination in yeast. Mol Cell Biol. 1998; 18:6525–6537. [PubMed: 9774668]

Chi P, Kwon Y, Seong C, Epshtein A, Lam I, Sung P, Klein HL. Yeast recombination factor Rdh54 functionally interacts with the Rad51 recombinase and catalyzes Rad51 removal from DNA. J Biol Chem. 2006; 281:26268–26279. [PubMed: 16831867]

Connolly B, White CI, Haber JE. Physical monitoring of mating type switching in Saccharomyces cerevisiae. Mol Cell Biol. 1988; 8:2342–2349. [PubMed: 2841579]

Datta A, Adjiri A, New L, Crouse GF, Jinks Robertson S. Mitotic crossovers between diverged sequences are regulated by mismatch repair proteins in Saccaromyces cerevisiae. Mol Cell Biol. 1996; 16:1085–1093. [PubMed: 8622653]

Deem A, Barker K, Vanhulle K, Downing B, Vayl A, Malkova A. Defective break-induced replication leads to half-crossovers in Saccharomyces cerevisiae. Genetics. 2008; 179:1845–1860. [PubMed: 18689895]

Deem A, Keszthelyi A, Blackgrove T, Vayl A, Coffey B, Mathur R, Chabes A, Malkova A. Break-induced replication is highly inaccurate. PLoS Biol. 2011; 9:e1000594. [PubMed: 21347245]

Donnianni RA, Symington LS. Break-induced replication occurs by conservative DNA synthesis. Proc Natl Acad Sci U S A. 2013; 110:13475–13480. [PubMed: 23898170]

Dresser ME, Ewing DJ, Conrad MN, Dominguez AM, Barstead R, Jiang H, Kodadek T. DMC1 functions in a Saccharomyces cerevisiae meiotic pathway that is largely independent of the RAD51 pathway. Genetics. 1997; 147:533–544. [PubMed: 9335591]

Forment JV, Kaidi A, Jackson SP. Chromothripsis and cancer: causes and consequences of chromosome shattering. Nat Rev Cancer. 2012; 12:663–670. [PubMed: 22972457]

Haber JE. Mating-type genes and MAT switching in Saccharomyces cerevisiae. Genetics. 2012; 191:33–64. [PubMed: 22555442]

Herskowitz I, Jensen RE. Putting the HO gene to work: practical uses for mating-type switching. Methods Enzymol. 1991; 194:132–146. [PubMed: 2005783]

Hicks WM, Kim M, Haber JE. Increased mutagenesis and unique mutation signature associated with mitotic gene conversion. Science. 2010; 329:82–85. [PubMed: 20595613]

Hicks WM, Yamaguchi M, Haber JE. Real-time analysis of double-strand DNA break repair by homologous recombination. Proc Natl Acad Sci U S A. 2011; 108:3108–3115. [PubMed: 21292986]

Holzen TM, Shah PP, Olivares HA, Bishop DK. Tid1/Rdh54 promotes dissociation of Dmc1 from nonrecombinogenic sites on meiotic chromatin. Genes Dev. 2006; 20:2593–2604. [PubMed: 16980587]

Ira G, Haber JE. Characterization of RAD51-independent break-induced replication that acts preferentially with short homologous sequences. Mol Cell Biol. 2002; 22:6384–6392. [PubMed: 12192038]

Ira G, Satory D, Haber JE. Conservative inheritance of newly synthesized DNA in double-strand break-induced gene conversion. Mol Cell Biol. 2006; 26:9424–9429. [PubMed: 17030630]

Kearney HM, Kirkpatrick DT, Gerton JL, Petes TD. Meiotic recombination involving heterozygous large insertions in Saccharomyces cerevisiae: formation and repair of large, unpaired DNA loops. Genetics. 2001; 158:1457–1476. [PubMed: 11514439]

Klein HL. RDH54, a RAD54 homologue in Saccharomyces cerevisiae, is required for mitotic diploid-specific recombination and repair and for meiosis. Genetics. 1997; 147:1533–1543. [PubMed: 9409819]

Lee SE, Pellicioli A, Malkova A, Foiani M, Haber JE. The Saccharomyces recombination protein Tid1p is required for adaptation from G2/M arrest induced by a double-strand break. Curr Biol. 2001; 11:1053–1057. [PubMed: 11470411]

Lydeard JR, Lipkin-Moore Z, Jain S, Eapen VV, Haber JE. Sgs1 and exo1 redundantly inhibit break-induced replication and de novo telomere addition at broken chromosome ends. PLoS Genet. 2010; 6:e1000973. [PubMed: 20523895]

Lyndaker AM, Goldfarb T, Alani E. Mutants defective in Rad1-Rad10-Slx4 exhibit a unique pattern of viability during mating-type switching in Saccharomyces cerevisiae. Genetics. 2008; 179:1807–1821. [PubMed: 18579504]

Malkova A, Ivanov EL, Haber JE. Double-strand break repair in the absence of RAD51 in yeast: a possible role for break-induced DNA replication. Proc Natl Acad Sci U S A. 1996; 93:7131–7136. [PubMed: 8692957]

Nickoloff JA, Sweetser DB, Clikeman JA, Khalsa GJ, Wheeler SL. Multiple heterologies increase mitotic double-strand break-induced allelic gene conversion tract lengths in yeast. Genetics. 1999; 153:665–679. [PubMed: 10511547]

Oldenburg KR, Vo KT, Michaelis S, Paddon C. Recombination-mediated PCR-directed plasmid construction in vivo in yeast. Nucleic Acids Res. 1997; 25:451–452. [PubMed: 9016579]

Pardo B, Aguilera A. Complex chromosomal rearrangements mediated by break-induced replication involve structure-selective endonucleases. PLoS Genet. 2012; 8:e1002979. [PubMed: 23071463]

Petukhova G, Sung P, Klein H. Promotion of Rad51-dependent D-loop formation by yeast recombination factor Rdh54/Tid1. Genes Dev. 2000; 14:2206–2215. [PubMed: 10970884]

Poli J, Tsaponina O, Crabbe L, Keszthelyi A, Pantesco V, Chabes A, Lengronne A, Pasero P. dNTP pools determine fork progression and origin usage under replication stress. Embo J. 2012; 31:883–894. [PubMed: 22234185]

Renkawitz J, Lademann CA, Kalocsay M, Jentsch S. Monitoring homology search during DNA double-strand break repair in vivo. Mol Cell. 2013; 50:261–272. [PubMed: 23523370]

Saini N, Ramakrishnan S, Elango R, Ayyar S, Zhang Y, Deem A, Ira G, Haber JE, Lobachev KS, Malkova A. Migrating bubble during break-induced replication drives conservative DNA synthesis. Nature. 2013; 502:389–392. [PubMed: 24025772]

Santa Maria SR, Kwon Y, Sung P, Klein HL. Characterization of the interaction between the Saccharomyces cerevisiae Rad51 recombinase and the DNA translocase Rdh54. J Biol Chem. 2013; 288:21999–22005. [PubMed: 23798704]

Schmidt KH, Wu J, Kolodner RD. Control of translocations between highly diverged genes by Sgs1, the Saccharomyces cerevisiae homolog of the Bloom's syndrome protein. Mol Cell Biol. 2006; 26:5406–5420. [PubMed: 16809776]

Shah PP, Zheng X, Epshtein A, Carey JN, Bishop DK, Klein HL. Swi2/Snf2-related translocases prevent accumulation of toxic Rad51 complexes during mitotic growth. Mol Cell. 2010; 39:862–872. [PubMed: 20864034]

Shinohara M, Gasior SL, Bishop DK, Shinohara A. Tid1/Rdh54 promotes colocalization of rad51 and dmc1 during meiotic recombination. Proc Natl Acad Sci U S A. 2000; 97:10814–10819. [PubMed: 11005857]

Signon L, Malkova A, Naylor ML, Klein H, Haber JE. Genetic requirements for RAD51- and RAD54-independent break-induced replication repair of a chromosomal double-strand break. Mol Cell Biol. 2001; 21:2048–2056. [PubMed: 11238940]

Smith CE, Llorente B, Symington LS. Template switching during breakinduced replication. Nature. 2007; 447:102–105. [PubMed: 17410126]

Spell RM, Jinks-Robertson S. Role of mismatch repair in the fidelity of RAD51- and RAD59-dependent recombination in Saccharomyces cerevisiae. Genetics. 2003; 165:1733–1744. [PubMed: 14704162]

Stafa A, Donnianni RA, Timashev LA, Lam AF, Symington LS. Template switching during break-induced replication is promoted by the Mph1 helicase in Saccharomyces cerevisiae. Genetics. 2014; 196:1017–1028. [PubMed: 24496010]

Sung P. Catalysis of ATP-dependent homologous DNA pairing and strand exchange by yeast RAD51 protein. Science. 1994; 265:1241–1243. [PubMed: 8066464]

Weiss K, Simpson RT. High-resolution structural analysis of chromatin at specific loci: Saccharomyces cerevisiae silent mating type locus HML alpha. Mol Cell Biol. 1998; 18:5392–5403. [PubMed: 9710623]

White CI, Haber JE. Intermediates of recombination during mating type switching in Saccharomyces cerevisiae. Embo J. 1990; 9:663–673. [PubMed: 2178924]

Yeeles JT, Poli J, Marians KJ, Pasero P. Rescuing stalled or damaged replication forks. Cold Spring Harb Perspect Biol. 2013; 5:a012815. [PubMed: 23637285]

Highlights

- Interchromosomal template switches (ICTS) occur in nearly 1% of DSB repair events
- ICTS is not impaired by heterochromatin
- Mismatch repair proteins Msh6 and Mlh1 direct strand-repair of heteroduplex DNA
- The chromatin remodeler Rdh54 is required for ICTS but not simple gene conversion

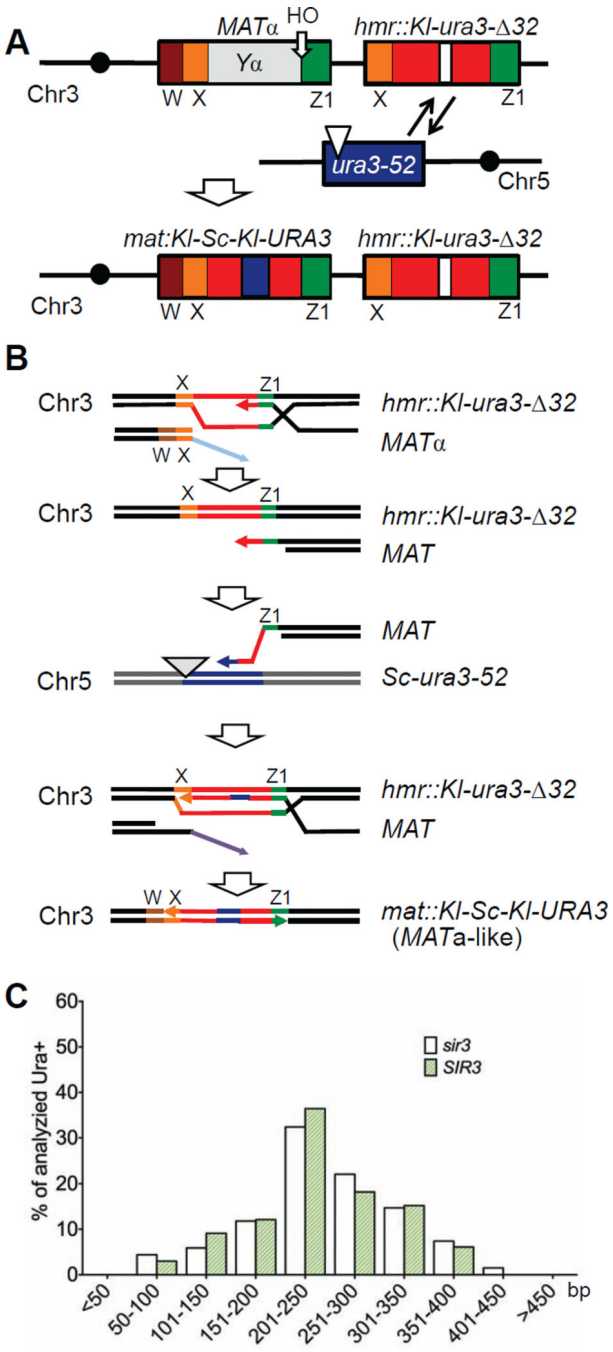

Figure 1. Selection of ICTS during gene conversion repair

A. Schematic representation of the ICTS assay used in this study. An HO endonuclease-induced DSB at *MAT*α initiates gene conversion repair with an *HMR* donor containing *K. lactis ura3* sequences with a 32-bp deletion. Rare ICTS events copy sequences from *S. cerevisiae ura3-52* and generate a Ura3^{+} chimeric sequence in *MAT*. Brown box: W region; orange box: X region; green box: Z1 region; red boxes separated by white box in *HMR* is *Ya::Kl-ura3-Δ32*. **B.** Proposed molecular events during ICTS. After the DSB is induced at *MAT*, the 5' to 3' resected end strand invades the *HMR* donor in the Z1 region of shared

homology and begins to copy the *Kl-ura3-Δ32* sequences. The nascent strand can dissociate and then anneal to ectopic homeologous *ura3-52* sequences on Chr5. After copying a small patch including the 32 bp missing in the *HMR* donor, the nascent strand dissociates again, anneals back to *HMR* and copies the remaining portion *Kl-ura3-Δ32* and at least part of the X sequences shared between *HMR* and *MAT*. The annealing of this nascent strand at *MAT* completes repair and results in a chimeric *Kl-Sc-Kl-URA3* gene. These Ura^+ outcomes can be selected on plates lacking uracil. **C**. Length of the copied *ura3-52* donor in *sir3Δ* (TOY43) and *SIR3* (TOY19) strains.

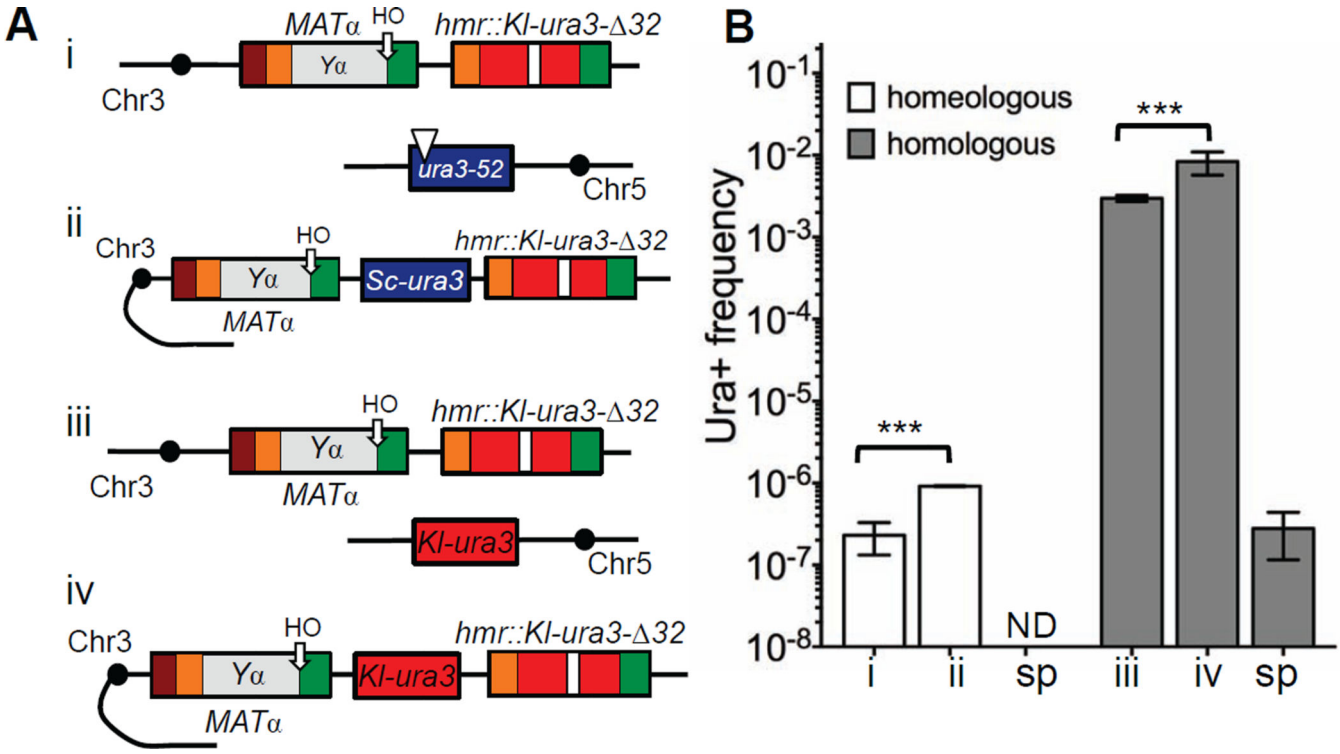

Figure 2. Increasing homology significantly promotes template switching during gene conversion

A. Analysis of Ura$^+$ rates in TOY43, TOY79, TOY47 and TOY74 strains. System was converted from inter- (i) to *intra*chromosomal (ii) template switches between two non-identical sequences. Interchromosomal template switches between two identical sequences can be studied by replacing *ura3-52* on Chr5 with *KI-ura3* sequences lacking both a promoter and the ATG start codon (iii). System to study *intra* chromosomal template switches between two identical sequences (iv). **B**. Analysis of template switches in strains described in **A**. sp = spontaneous. ND = not detected; less than 1×10^{-10}. Data are represented as mean +/− SEM.

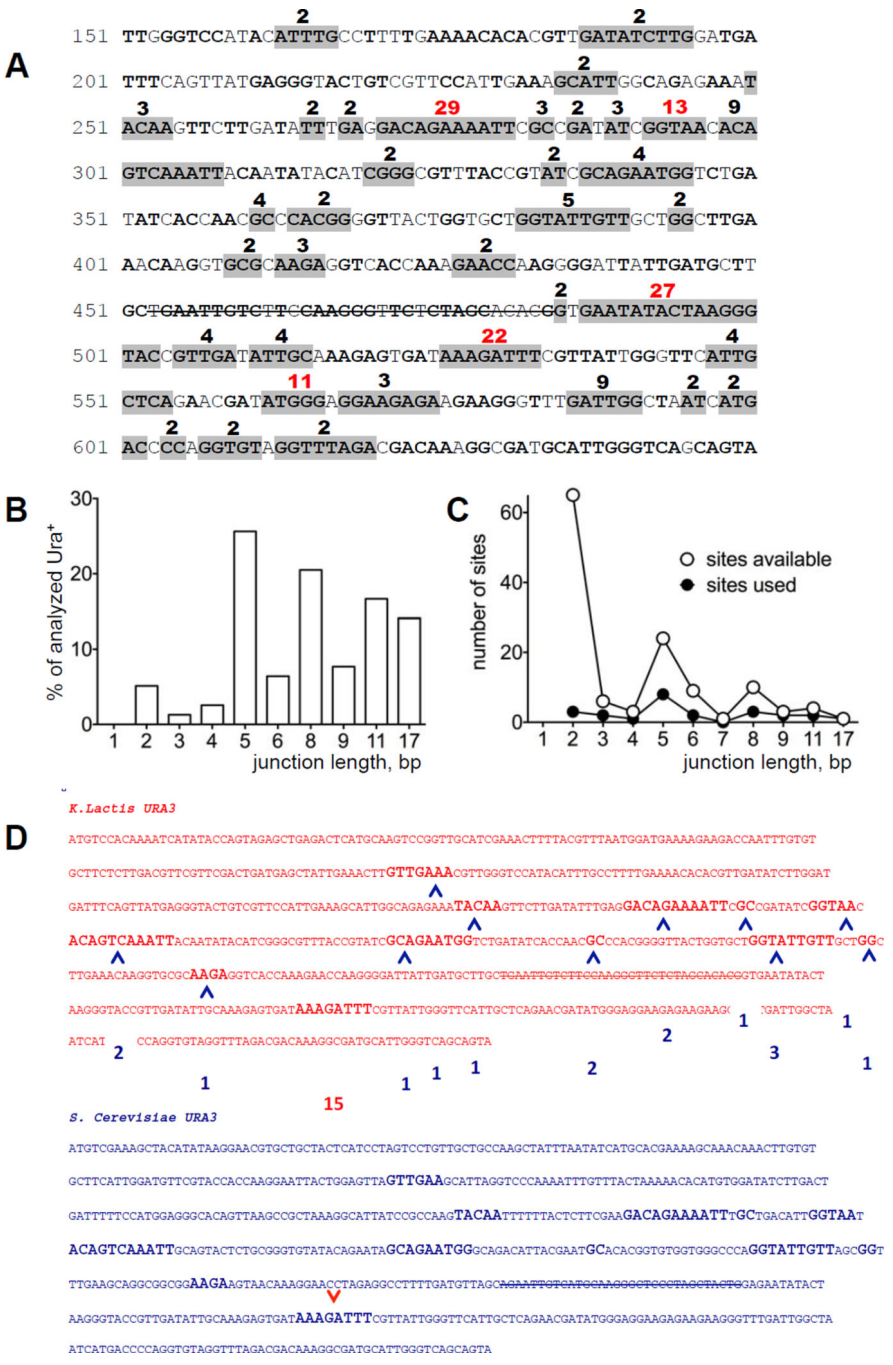

Figure 3. A number of microhomologies are used for ICTS

A. Sequence of *K. lactis URA3* from 150 to 650 bp. In-frame, shared microhomologies between *Kl-URA3* and *Sc-URA3* are in **bold**. Gray-highlighted microhomologies were found among 94 Ura$^+$ colonies in *sir3*Δ strain (TOY43). The strike-through sequence represents the 32-bp deletion (Δ*32*). Numbers over the sequence are the percentage of microhomology usage among the Ura$^+$ colonies analyzed. The five most frequently used sites are shown in red. **B.** Length distribution of microhomologies shown in **A. C.** Distribution of available shared microhomologies between *Kl-URA3* and *Sc-URA3*. Open circles illustrate the number

of possible junctions of a particular length; filled circles represent the number of different junctions of each particular length used for template switches. **D.** Among 15 template switches involving one specific 3’ junction (red arrow), a second template switch occurred at each of the indicated 5’ junctions (blue arrows), with their frequency of usage shown in blue boxes.

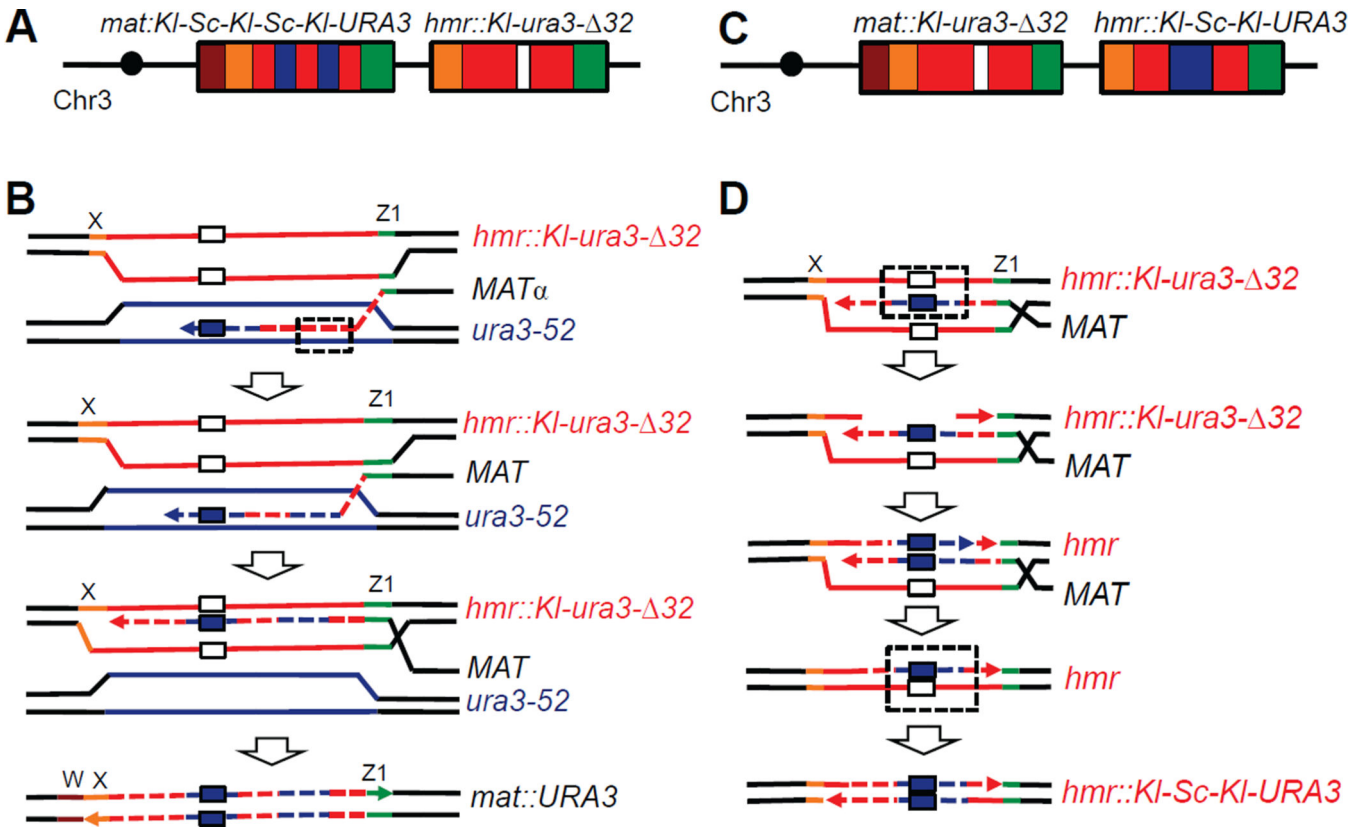

Figure 4. Msh6 is crucial for strand discrimination during interchromosomal template switch

A. Multiple *Sc-ura3* patches identified in a Ura$^+$ at *MAT* in a *msh6*Δ strain (TOY44). **B.** Scheme illustrating appearance of a *Kl-Sc-Kl-Sc-Kl* pattern in a *URA3* chimeric gene in *MAT*. When the nascent repair strand dissociates from *HMR* and anneals to *ura3-52* on Chr5, a heteroduplex DNA (hDNA) is formed (dashed box). hDNA is recognized and corrected by Msh6-independent mismatch repair using the *ura3-52* strand as a template. **C**. A footprint of *ura3-52* was also found replacing the 32-bp deletion at *hmr::Kl-ura3-*Δ*32* in some *sir3*Δ cells lacking Msh6 and/or Mlh1. **D**. A possible explanation of *ura3-52* footprint in *HMR*. The nascent repair strand dissociates from *HMR* and copies a patch from the ectopic donor, including the 32-bp segment on Chr5. After re-invasion into *HMR*, hDNA is formed (dashed box) which is recognized and used by mismatch repair to replace the deleted 32-bp segment and create an expressed chimeric *URA3* gene. Such events were only found in *msh6* and/or *mlh1* cells that apparently are not able to discriminate the intact from the invading strand. White box: Δ*32*; dark blue box: sequence corresponding Δ*32* copied from *Sc-ura3-52*.

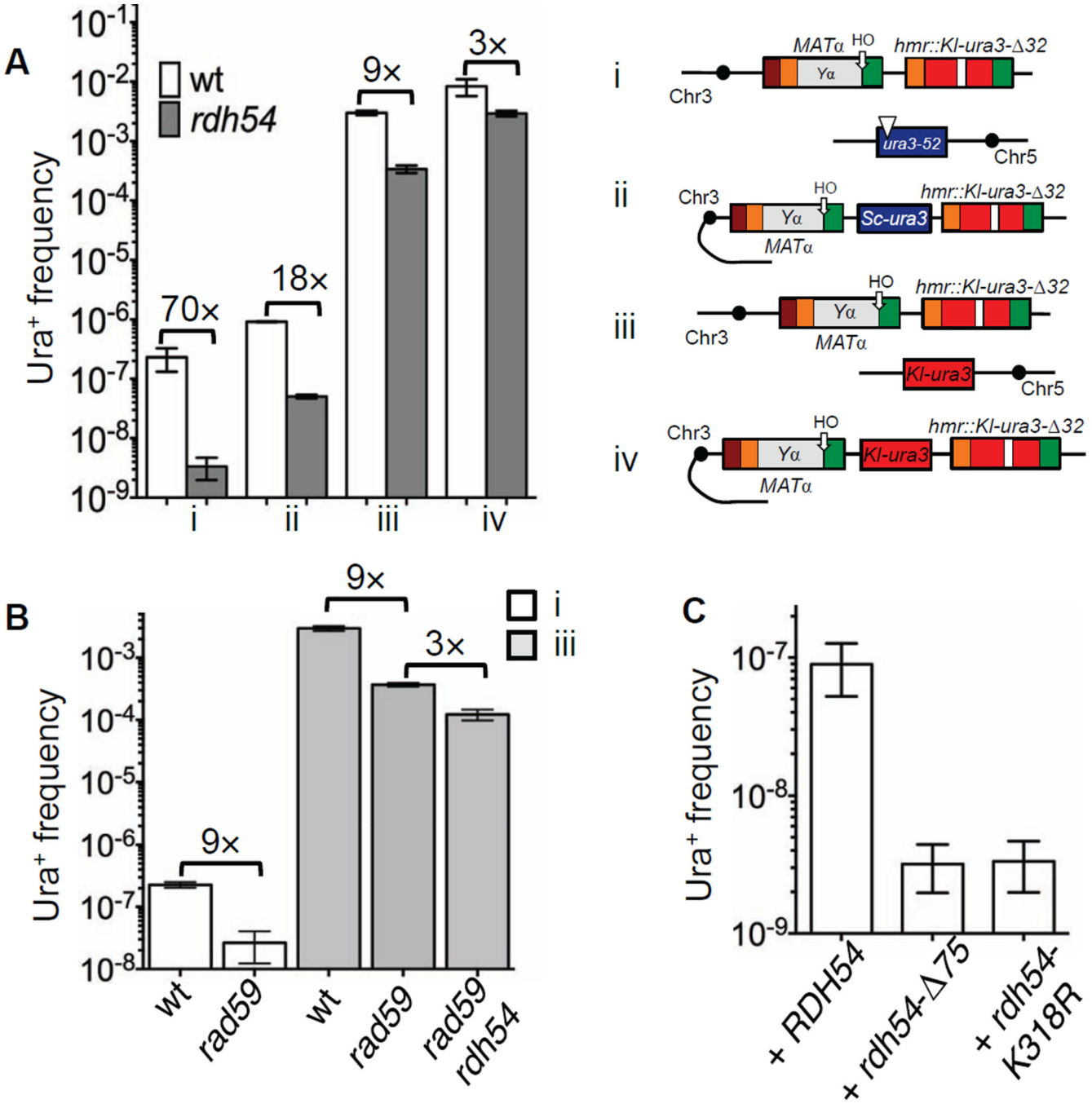

Figure 5. Rdh54 is important for template switching

A. In an *rdh54*Δ strain, template switching between inter- (TOY62) and intachromosomal (TOY83) homeologous sequences is reduced 70-fold and 18-fold correspondingly compared to the wild type (i and ii). Deletion of *RDH54* also reduces homologous template switching 10-fold to 3×10^{-4} (TOY64) (iii) and has a similar effect on intrachromosomal homologous events reducing rates to the 3×10^{-3} (TOY77) (iv). **B**. Analysis of Ura^+ rates in TOY43, TOY47, TOY85, TOY90 and TOY91 strains. In *rad59*Δ strain, frequency of ICTS both between homeologous and homologous templates is reduced compared to wild type

(compare i and iii). Absence of Rad59 in *rdh54*Δ further decreases ICTS even for homologous system. **C**. Both ATPase activity of Rdh54 and its interaction with Rad51 are required for ICTS. Data are represented as mean +/− SEM.

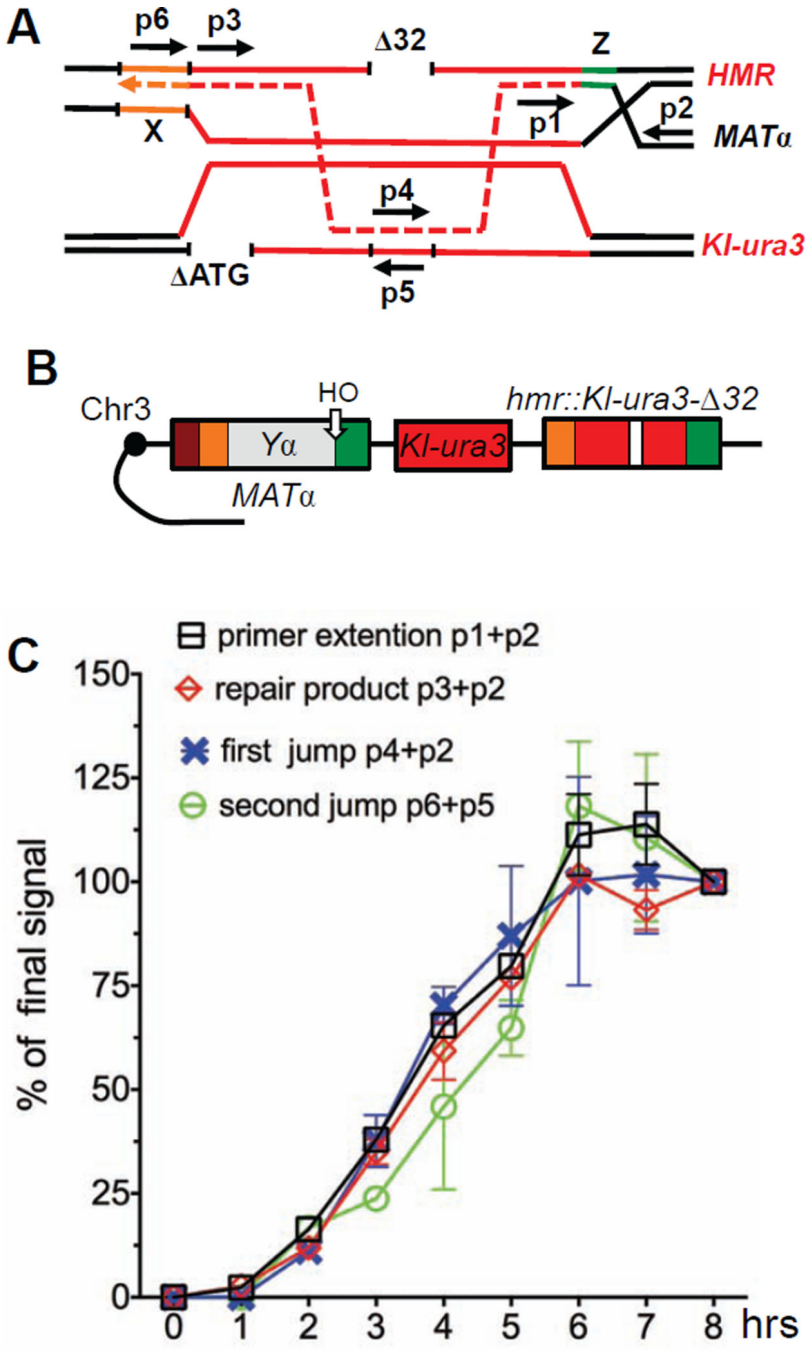

Figure 6. Kinetics of template switching between homologous sequences

A. Primers used to analyze the kinetics of simple gene conversion repair and template switch. **B.** Template switching strains to analyze homologous intrachromosomal events (TOY74). **C**. Kinetics of gene conversion repair and template switch in TOY74. Data are represented as mean +/− SEM.

Table 1

Rate of interchromosomal template switches, average length of copied ectopic donor and average length of 3’ and 5’ junction sites in different strains*

	Genotype	Rate of ICTS, $\times 10^{-7}$ **	Relative rate of ICTS versus wild type	Average length of copied *ura3-52*	Average length of 5’ junction (bp)	Average length of 3’ junction (bp)	Number of Ura^+ clones analyzed
	*sir3*Δ	2.3 ± 0.1	na	247 ± 9	7.3 ± 0.4	9.2 ± 0.6	94
	SIR3	1.4 ± 0.4	0.6	246 ±10	8.7 ± 0.5	9.4 ± 0.7	48
helicase	*sgs1*Δ	2.4 ± 0.3	1.0	253 ± 9	8.0 ± 0.5	9.4 ± 0.7	48
	*mph1*Δ	2.5 ± 0.2	1.1	258 ± 11	9.5 ± 0.5	11.3 ± 1.0	48
	*sgs1*Δ *mph1*Δ	3.3 ± 0.3	1.4	269 ± 8	9.0 ± 0.4	9.9 ± 0.6	59
MMR	*mlh1*Δ	5.2 ± 0.9	2.3	245 ± 6	7.4 ± 0.4	10.4 ± 0.6	96
	*msh3*Δ	3.7 ± 0.7	1.6	250 ± 7	7.8 ± 0.4	10.0 ± 0.6	96
	*msh6*Δ	4.8 ± 0.8	2.1	231 ± 10	6.9 ± 0.4	8.6 ± 0.6	70
	*msh6*Δ *msh3*Δ	3.1 ± 0.2	1.3	233 ± 6	7.6 ± 0.4	11.3 ± 0.5	92
	*msh6*Δ *mlh1*Δ	2.7 ± 0.6	1.2	247 ± 12	7.4 ± 0.3	10.1 ± 0.6	94
	*rad1*Δ	1.1 ± 0.2	0.5	239 ± 8	7.6 ± 0.3	10.9 ± 0.6	92
double mutant	*msh6*Δ *mph1*Δ	10.0 ± 1.2	4.3	242 ± 15	7.8 ± 0.5	9.8 ± 0.7	48
	*msh6*Δ *rad1*Δ	2.7 ± 0.5	1.2	264 ± 9	7.9 ± 0.4	9.8 ± 0.7	68

* all strains are *sir3*Δ unless otherwise noted;

** p-values >0.05